Global Journal of Engineering and Technology Advances
eISSN: 2582-5003
Cross Ref DOI: 10.30574/gjeta
Journal homepage: https://gjeta.com/

(RESEARCH ARTICLE)

Check for updates

COUPLED NONLINEAR HEAVE–PITCH MOTION MODEL FORMULATION AND HYDRODYNAMIC CHARACTERIZATION

Tamunosiki Promise Christian *, Samson Nitonye and King Nyeche Wugha

Department of Marine and Offshore Engineering, Faculty of Engineering, Rivers State University, Nkpolu-Oroworukwo, Port Harcourt, Nigeria.
* Corresponding Author

ORCID Details
Tamunosiki Promise Christian: https://orcid.org/0009-0003-1844-1920

Global Journal of Engineering and Technology Advances, 2026, 29(01), 351–365

Publication history: Received on 17 September 2026; revised on 24 October 2026; accepted on 26 October 2026

Article DOI: https://doi.org/10.30574/gjeta.2026.29.1.0306

Copyright © 2026 Author(s) retain the copyright of this article. This article is published under the terms of the Creative Commons Attribution License 4.0

ABSTRACT

In this study, Coupled Nonlinear Heave–Pitch Motion Model Formulation and Hydrodynamic Characterization was carried out to investigate the interaction between vertical displacement and angular rotation of a ship under irregular wave conditions. Excessive heave and pitch motions can affect vessel stability, structural safety, cargo operations, and seakeeping performance. The research focused on developing a coupled nonlinear mathematical model for a Series 60 ship hull using frequency-dependent added mass, radiation damping, hydrostatic restoring forces, nonlinear restoring terms, and wave excitation forces. Unlike studies focusing mainly on linear motion prediction or individual response characteristics, this study incorporates cubic nonlinear restoring terms and hydrodynamic coefficients obtained from ANSYS AQWA for comparison. The Pierson–Moskowitz spectrum was adopted to represent irregular waves with a significant wave height of 7.45 m and a zero-crossing period of 10 s. The AQWA results recorded peak heave and pitch response amplitude operators (RAOs) of 1.019 m/m and 2.380°/m, respectively, under 180° head seas. Heave added mass decreased from 23.4×10^6 kg at 0.3 rad/s to 7.36×10^6 kg at 1.4 rad/s, representing a 68.5% reduction. Heave radiation damping peaked at 7.24×10^5 Ns/m at 0.8 rad/s. At 3 m heave displacement, nonlinear restoring force increased by 19.4% above the linear value, while pitch restoring moment increased by 6.6% at 0.30 rad. These results demonstrate that nonlinear effects become more significant at larger motion amplitudes. The developed model contributes a mathematical basis for ship-motion assessment and supports improved seakeeping analysis. Further time-domain simulation and validation against AQWA response predictions are recommended to establish model accuracy under severe sea conditions.

Keywords: Added mass; Radiation damping; Restoring stiffness; Irregular waves; Response amplitude operators

1 INTRODUCTION

Ships operating in the sea are exposed to waves that cause different types of motion, which can affect their stability, safety, and performance. Two important types of ship motion are heave and pitch. Heave is the vertical movement of a ship, while pitch is the rotation of the ship about its transverse axis. These motions are important in ship design because large movements can affect cargo handling, passenger comfort, structural strength, and offshore operations. According

to Yu et al. (2021), wave-induced ship motions are affected by wave conditions and the movement of the vessel. Recent research by Wang et al. (2025) also examined the nonlinear heave and pitch motions of ships in head seas. These studies show the need to understand how ships respond to waves, especially when the wave forces produce large and complex movements.

Heave and pitch motions are influenced by the ship's mass, shape, speed, added mass, damping, and hydrostatic restoring forces. Added mass refers to the additional water that moves with the ship during its motion, while damping describes the loss of motion energy caused by the interaction between the ship and the surrounding water. Restoring forces act to return the ship towards its equilibrium position after it has been displaced. These forces and moments may interact, meaning that heave motion can influence pitch motion and vice versa. Although linear models are useful for studying ship motions, they may not fully describe the behaviour of a ship when the motion becomes large. Nonlinear restoring forces and damping terms can help explain changes in the ship's response at larger motion amplitudes (Faltinsen, 1990; Fossen, 2011). Therefore, a coupled nonlinear model is important for studying the relationship between heave and pitch under different wave conditions.

Several studies have examined ship motion prediction and hydrodynamic analysis using mathematical models and numerical methods. Yu et al. (2021) developed a model for studying ship motions during turning in regular and irregular waves. Their findings showed that the predicted motions could agree with experimental results under some wave conditions, although differences remained for certain irregular wave cases. Schirmann et al. (2022) examined methods for predicting vessel motions and showed the importance of including physical information in motion prediction. In another study, La Ferlita et al. (2024) compared different methods for predicting ship responses and assessed their performance using numerical and experimental results. More recently, Yu et al. (2026) assessed the open-source NEMOH hydrodynamic model against ship motion measurements and reported good agreement for heave, while some differences remained in pitch and roll under certain severe sea conditions. Wang et al. (2025) also investigated the nonlinear heave and pitch motions of a ship in head seas. Although these studies have improved the understanding of ship motions, differences in their methods, operating conditions, and levels of validation show the need for further investigation of coupled nonlinear motion models and their hydrodynamic behaviour. Recent numerical studies have also assessed vessel hydrodynamic characteristics under region-specific environmental conditions and across different hull configurations (Chuku et al., 2026; Oludi & Nwoka, 2025). Related offshore hydrodynamic research has combined frequency-domain response analysis with time-domain verification to identify resonant pitch behaviour; although that work concerns a tension-leg floating wind platform rather than a conventional ship hull, its treatment of frequency-dependent response is relevant to the present analysis (Ekine et al., 2026). Recent numerical studies have assessed vessel hydrodynamic characteristics under region-specific environmental conditions and across different hull configurations (Chuku et al., 2026; Oludi & Nwoka, 2025).

Related offshore hydrodynamic research has combined frequency-domain response analysis with time-domain verification to identify resonant pitch behaviour. Although that work concerns a tension-leg floating wind platform rather than a conventional ship hull, its treatment of frequency-dependent response is relevant to the present analysis (Ekine et al., 2026).

A mathematical model that combines heave and pitch motions can help explain how these motions interact under wave excitation. In this study, the Series 60 ship hull will be used to develop and examine a coupled nonlinear heave–pitch motion model. The model will include the ship's mass and pitch moment of inertia, frequency-dependent added mass and radiation damping, hydrostatic restoring forces, nonlinear restoring terms, and wave excitation forces and moments. The study will also consider irregular waves represented by the Pierson–Moskowitz wave spectrum. ANSYS AQWA will be used to obtain hydrodynamic coefficients and response amplitude operators (RAOs) for comparison with the developed model. This comparison will help assess whether the model can reproduce the main heave and pitch response characteristics of the selected ship. The use of an established ship hull and an independent numerical reference will support a systematic assessment of the model's behaviour.

Despite the progress made in ship motion analysis, there is still a need to examine how nonlinear restoring forces and the interaction between heave and pitch affect ship response under irregular wave conditions. Some existing studies focus on linear response analysis, individual motion characteristics, or specific operating conditions, while the combined effects of nonlinear restoring forces and coupled motion require further examination. The present study will address this need by formulating a coupled nonlinear heave–pitch motion model for a Series 60 ship hull and examining its hydrodynamic behaviour under wave excitation. The model will be assessed using hydrodynamic coefficients and response amplitude operators obtained from ANSYS AQWA. The study is expected to improve the understanding of coupled heave and pitch motions and contribute to the mathematical analysis of ship responses in waves.

2 MATERIAL AND METHOD

2.1 Vessel Parameters and Data Source

The vessel data used in this study include the principal dimensions, hydrostatic characteristics, mass properties and other parameters required for the analysis of ship heave and pitch motions. The vessel is based on a benchmark Series 60 ship hull commonly used in ship hydrodynamic studies. The principal parameters include length between perpendiculars, breadth, draft, depth, displacement, block coefficient, mass, radius of gyration and pitch moment of inertia.

The importance of defining the principal dimensions is also reflected in comparative vessel-resistance research, which examines how changes in hull length affect hydrodynamic resistance (Nwoka et al.,

The vessel geometry was prepared for hydrodynamic analysis using ANSYS AQWA. The AQWA analysis provided independent hydrodynamic and response information, including added mass, radiation damping, hydrostatic restoring stiffness and Response Amplitude Operators (RAOs) for heave and pitch. These results are used as reference results for assessing the behaviour of the nonlinear stochastic model developed in this study. The AQWA analysis gave a peak heave RAO of 1.019 m/m and a peak pitch RAO of 2.380°/m for the 180° head-sea condition.

The vessel design information and hydrodynamic results used in the study were obtained from the vessel data and the ANSYS AQWA analysis carried out for the study. The main mathematical work consists of formulating the coupled nonlinear heave–pitch equations, converting them into stochastic differential equations, and solving them numerically. ANSYS AQWA is used as a hydrodynamic reference for assessing the developed model. The vessel considered in this study is the Series 60 ship model.

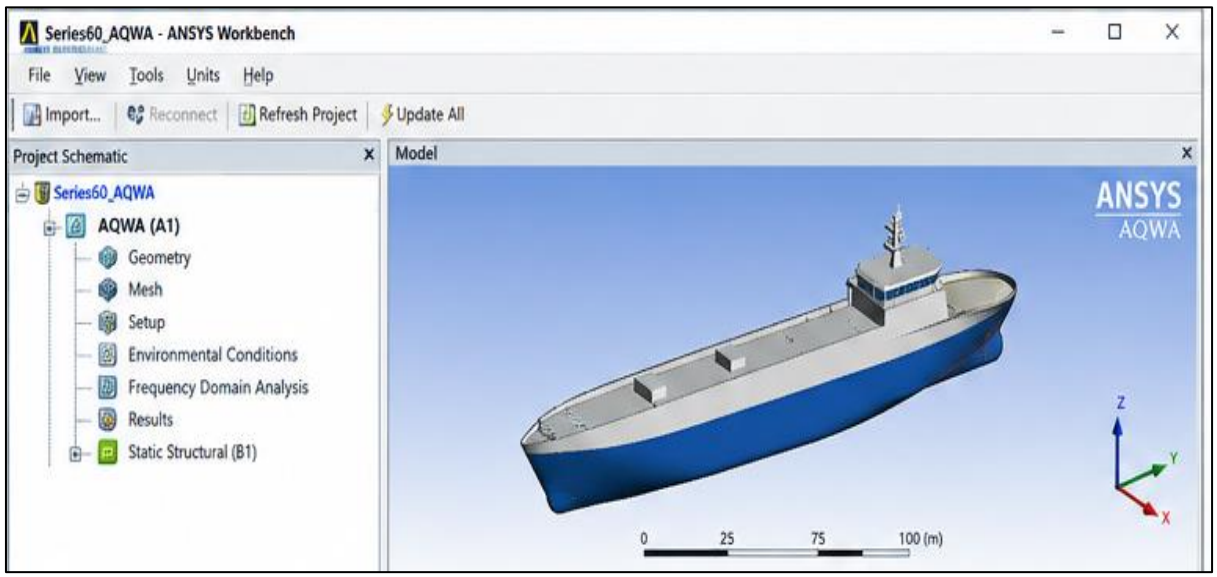


Figure 1: ANSYS AQWA Workbench Project tree and Series 60 vessel model

Table 1: Principal Ship parameters

Parameter	Symbol	Typical value	Unit
Length between perpendiculars	L_{pp}	121.92	m
Breadth	B	16.46	m
Draft	T	6.86	m
Depth	D	10.20	m
Block coefficient	C_B	0.70	-
Water-plane coefficient	C_w	0.82	-
Prismatic coefficient	C_p	0.72	-
Displacement volume	∇	9518.6	m^3
Ship mass used in AQWA	M	9.76×10^6	Kg
Radius of gyration in pitch	K_{yy}	30.38	m
Pitch moment of inertia	I_{yy}	9.005×10^9	$Kg.m^2$
Metacentric height	GM	1.8	m
Heave restoring coefficient	K_{33}	1.662×10^7	N/m
Pitch restoring coefficient	K_{55}	2.568×10^8	Nm/rad
Forward speed	U	10	Knots
Gravity	G	9.80665	m/s^2
Water depth	H	1000	M
Water density	ρ	1025	Kg/m^3

Source: Todd, F.H. (1953). "Series 60: Systematic Experiments with Models of Single-Screw Merchant Ships." David Taylor Model Basin Report No. 1712, U.S. Navy, Washington D.C.

The ship mass, m is required because it determines the resistance of the vessel to acceleration in heave. The pitch moment of inertia, I_{yy} describes the resistance of the vessel to angular acceleration during pitch motion. The radius of gyration, K_{yy} describes the distribution of the ship's mass about the pitch axis.

The water density, ρ and gravitational acceleration, g, are required in calculating the hydrodynamic and hydrostatic forces acting on the vessel. The metacentric height, GM provides information about the vessel's stability and contributes to the restoring characteristics of the ship.

These parameters are needed to establish the physical properties of the vessel before developing the coupled heave-pitch model.

2.1.1 Ship Geometry and Computational Model

The geometry of the Series 60 hull was prepared to provide the physical representation of the vessel used in the hydrodynamic analysis. The geometry was also used as the basis for the computational representation of the hull.

2.1.1.1 Description of the Series 60 Hull

The vessel used in this study is based on the Series 60 ship hull, which is a standard benchmark hull used in ship hydrodynamic and seakeeping studies. The hull was selected because its principal dimensions and geometric characteristics provide a suitable basis for investigating ship motions in waves.

The principal dimensions of the vessel used in the study are presented in Table 3.1. These dimensions define the overall size and form of the vessel used in the mathematical and hydrodynamic analyses.

2.1.1.2 Hull Geometry Development

The hull geometry was developed from the principal dimensions of the Series 60 vessel and prepared for computational hydrodynamic analysis. The geometry represents the underwater hull surface required for the hydrodynamic calculations.

The developed geometry was used to establish the computational representation of the vessel. The geometry was subsequently prepared for panelization so that the hull surface could be represented by computational elements during the AQWA analysis.

2.1.1.3 Coordinate System and Reference Points

A ship-fixed coordinate system was used to describe the position and orientation of the vessel. The longitudinal direction represents the length of the vessel, the transverse direction represents the breadth, and the vertical direction represents the depth.

The vertical displacement of the vessel is represented by z, while the rotation about the transverse axis is represented by θ. These two variables are used to describe the heave and pitch motions considered in the study.

2.1.1.4 Computational Representation of the Hull

The developed hull geometry was converted into a computational representation for hydrodynamic analysis. This representation allows the underwater hull surface to be divided into computational elements through which the interaction between the vessel and the surrounding water can be evaluated.

The computational model was used in ANSYS AQWA to obtain the independent hydrodynamic information required for comparison with the mathematical model.

2.1.1.5 Panelization and Mesh Generation

The hull surface was discretized into computational panels to form the mesh used in the hydrodynamic analysis. Panelization provides a numerical representation of the hull surface required by the hydrodynamic solver.

The computational mesh was therefore generated before the AQWA analysis. The resulting panel model was used to calculate the hydrodynamic properties and ship-response characteristics that were later used for validation.

2.2 Hydrodynamic Analysis Using ANSYS AQWA

ANSYS AQWA was used to obtain independent hydrodynamic and ship-response information for validation of the mathematical model. The analysis considered the Series 60 hull under the specified vessel and environmental conditions.

The hydrodynamic analysis provides information on the interaction between the vessel and the surrounding water. The quantities of interest include added mass, radiation damping, hydrostatic restoring stiffness and response amplitude operators for the heave and pitch motions.

For the 180° head-sea condition, the AQWA frequency-domain analysis gave a maximum heave RAO of 1.019 m/m and a maximum pitch RAO of 2.380°/m.

The available AQWA results also provided a heave added-mass range of approximately 7.36×10^{6} to 2.34×10^{7}kg, together with frequency-dependent damping and restoring information. These values provide independent hydrodynamic information for comparison with the model.

AQWA is needed in this study because it provides an independent numerical reference for the vessel's hydrodynamic behaviour. The developed stochastic model must produce physically reasonable ship motions. Therefore, its predictions can be compared with AQWA results under the same or equivalent vessel and sea conditions. This gives a basis for assessing whether the developed model can reproduce the important characteristics of ship heave and pitch motion.

2.2.1 Derivation of the Velocity Potential and wave Elevation

The wave field surrounding the vessel is described using the velocity potential approach. The fluid is assumed to be incompressible, inviscid and irrotational. Under these assumptions, the fluid velocity can be expressed in terms of a velocity potential ϕ (x, z, t) as

$$u = \frac{\partial \phi}{\partial x}, \qquad w = \frac{\partial \phi}{\partial z} \tag{1}$$

(Newman, 1977; Dean & Dalrymple, 1991)

where u and w are the horizontal and vertical components of fluid velocity, respectively.

For an incompressible fluid, the continuity equation is

$$\frac{\partial u}{\partial x} + \frac{\partial w}{\partial z} = 0 \tag{2}$$

Substituting the velocity components in terms of the velocity potential gives the expanded Laplace equation:

$$\frac{\partial^2 \phi}{\partial x^2} + \frac{\partial^2 \phi}{\partial z^2} = 0 \tag{3}$$

Therefore, the velocity potential satisfies Laplace's equation:

$$\nabla^2 \phi = 0 \tag{4}$$

For a progressive regular wave, the velocity potential is assumed to have the form

$$\phi(x, z, t) = F(z) \sin(kx - \omega t), \tag{5}$$

Where k is the wave number and ω is the angular frequency.

Substitution into Laplace's equation gives

$$F''(z) - k^2 F(z) = 0 \tag{6}$$

The general solution is

$$F(z) = Ae^{kz} + Be^{-kz} \tag{7}$$

For a fluid of finite depth h, the vertical velocity at the seabed must be zero. Therefore, the bottom boundary condition is

$$\frac{\partial \phi}{\partial z} = 0 \qquad at\ z = -h \tag{8}$$

Applying this condition gives the vertical dependence in the form

$$F(z) = Ccoshk(z + h) \tag{9}$$

Hence, the finite velocity potential can be written as

$$\phi(x, z, t) = Ccoshk(z + h) \sin(kx - \omega t), \tag{10}$$

The free-surface boundary conditions are then applied at the mean water surface z=0

The linearized kinematic free-surface boundary condition is

$$\frac{\partial \eta}{\partial t} = \frac{\partial \eta}{\partial z} \qquad at\ z = 0 \tag{11}$$

$\eta(x, t)$ is the wave elevation.

The linearized dynamic free-surface boundary condition is

$$\frac{\partial \phi}{\partial t} + g\eta = 0 \quad at\ z = 0 \tag{12}$$

The wave elevation is represented by

$$\eta(x,t) = \text{acos}(kx - \omega t) \quad (13)$$

Where a is the wave amplitude.

Using the dynamic free-surface boundary condition gives the relationship,

$$\frac{\partial \eta}{\partial t} = -g\eta \quad (14)$$

Substitution of the harmonic wave elevation and integration with respect to time gives the finite-depth velocity potential after applying conditions

$$\phi(x,z,t) = \frac{ag}{\omega}\frac{Ccoshk(z+h)}{coshkh}\sin(kx - \omega t), \quad (15)$$

This expression describes the velocity potential associated with a linear progressive surface wave in water of finite depth.

For deep water approximation, where the water depth is sufficiently large compared with the wavelength,

$$\frac{coshk(z+h)}{coshkh} \approx e^{kz} \quad (16)$$

Therefore, the deep-water velocity potential becomes

$$\phi(x,z,t) = \frac{ag}{\omega}e^{kz}\sin(kx - \omega t), \quad (17)$$

The relationship between the velocity potential and the wave elevation is obtained directly from the dynamic free-surface boundary condition as

$$\eta = -\frac{1}{g}\frac{\partial \phi}{\partial t} \quad (18)$$

The kinematic and dynamic boundary conditions can also be combined to obtain the wave dispersion relationship:

$$\omega^2 = gktanh(kh) \quad (19)$$

For deep water, the dispersion relationship reduces to

$$\omega^2 = gk \quad (20)$$

The pressure associated with the wave field can be obtained from the linearized Bernoulli equation:

$$p = -\rho\left(\frac{\partial \phi}{\partial t} + gz\right) \quad 21$$

Thus, the velocity potential provides the fluid velocity and pressure associated with the wave field, while the wave elevation describes the corresponding displacement of the free surface (linearized pressure equation). These relationships provide the theoretical basis for representing the wave excitation acting on the vessel in the coupled heave–pitch motion model. "The formulation presented in Equations (1) – (21) is adapted from the established linear wave theory of Newman (1977) and Dean and Dalrymple (1991)."

2.3 Formulation of the Coupled Nonlinear Heave-Pitch Motion Model

The vertical motion of the vessel is represented by two coupled degrees of freedom: heave and pitch. Heave represents the vertical displacement of the vessel denoted by z, while pitch represents its angular rotation about the transverse axis and is denoted by θ. The corresponding velocities are $\dot{z}$ and $\dot{\theta}$. The two motions are coupled because the hydrodynamic forces and moments associated with one mode can influence the other.

The displacement vector is defined as

$$x(t) = \begin{bmatrix} z \\ \theta \end{bmatrix}, \quad (22)$$

Where; z is the heave displacement and θ is pitch angle.

The coupled nonlinear equations of motion used in this study were adapted from established ship-motion and marine dynamics formulations (Salvesen, Tuck, & Faltinsen, 1970; Faltinsen, 1990; Newman, 1977). The standard formulation was modified to suit the present study, which focuses on the coupled heave and pitch motions of the Series 60 ship model in head seas. The modifications include the inclusion of nonlinear restoring terms in heave and pitch and the use of wave-excitation force and moment obtained from the hydrodynamic analysis. The hydrodynamic coefficients used in the model were obtained from the ANSYS AQWA analysis. Nonlinear restoring effects have also been considered in nonlinear ship-motion models (Ibrahim & Grace, 2010; Neves et al., 2006).

The general coupled nonlinear equations of motion are written as:

$$M\ddot{x} + B(\dot{x}) + C(x) + N(x) = F_w(t) \quad (23)$$

Where:

M = the mass matrix including the ship mass, pitch moment of inertia, and added-mass terms

B = damping force and moments

C = the linear hydrostatic restoring forces and moments

N = nonlinear restoring and damping terms

$F_{wave}(t)$ = the wave excitation force and moment vector acting on the vessel.

x =displacement vector containing heave and pitch motions

2.3.1 Mass and Added-Mass Matrix

The effective mass matrix for the coupled heave-pitch model is expressed as:

$$M = \begin{bmatrix} m + A_{33} & A_{35} \\ A_{53} & I_{yy} + A_{55} \end{bmatrix} \quad (24)$$

(Adapted from Salvesen *et al*., 1970; Journée & Massie, 2001)

Where;

m = the ship mass

I_{yy} = the pitch moment of inertia about the transverse axis,

A_{33}= added mass associated with heave motion

A_{35} , A_{53}= coupling added-mass coefficients between heave and pitch.

A_{55}= added-mass coefficients for pitch motion

The added-mass terms represent the additional inertia caused by the surrounding water. They are important because part of the surrounding water moves with the vessel during its motion. The hydrodynamic values used for comparison were obtained from the AQWA analysis.

2.3.2 Damping

The damping terms represent forces and moments that oppose the vessel's motion and remove energy from the system. In the present model, damping may contain both linear and nonlinear components. The damping matrix was adapted from established ship-motion formulations and modified for the present coupled heave-pitch model. The damping coefficients used in the present study were obtained from the AQWA hydrodynamic analysis.

The damping matrix is written as

$$B = \begin{bmatrix} B_{33} & B_{35} \\ B_{53} & B_{55} \end{bmatrix} \quad (25)$$

Where;

B_{33} = heave radiation damping coefficient

B_{55} = pitch radiation damping coefficient

$B_{35}\ and\ B_{53}$ = coupling damping coefficients. These terms represent the energy dissipated through the interaction between the moving vessel and the surrounding water.

The restoring matrix is expressed as

$$C = \begin{bmatrix} C_{33} & C_{35} \\ C_{53} & C_{55} \end{bmatrix} \quad (26)$$

Where;

C_{33} = heave restoring coefficient

C_{55} = pitch restoring coefficient

$C_{35}\ and\ C_{53}$ = hydrostatic coupling terms.

The nonlinear restoring contribution is represented by

$$N(x) = \begin{bmatrix} \alpha z^3 \\ \beta \theta^3 \end{bmatrix}, \quad (27)$$

Where;

α = nonlinear restoring coefficient for heave

β = nonlinear restoring coefficient for pitch

$z^3\ and\ \theta^3$ = nonlinear contribution to the restoring force and moment. The inclusion of these terms allows the model to represent motion behaviour beyond a purely linear restoring relationship.

The external wave excitation force and moment vector is represented by

$$F(t) = \begin{bmatrix} F_3(t) \\ M_5(t) \end{bmatrix}, \quad (28)$$

(Faltinsen, 1990; Jensen *et al*., 2004).

Where;

$F_3(t)$ = wave excitation force in heave

$M_5(t)$ = wave excitation moment in pitch

Therefore, the individual coupled equations can be written as

For heave, the nonlinear damping force can generally be represented as

$$C_z(\dot{z}) = C_z(\dot{z}) + C_{z3}\dot{z}^{\,3} \quad (29)$$

While the nonlinear pitch damping moment can be represented as

$$C_\theta(\dot{\theta}) = C_4(\dot{\theta}) + C_{\theta 3}\dot{\theta}^{\,3} \quad (30)$$

The linear terms represent ordinary viscous/radiation damping, while the higher-order terms allow nonlinear damping effects to be considered.

2.3.3 Restoring forces

The restoring terms act to return the vessel towards its equilibrium position after displacement.

For heave and pitch, the nonlinear restoring forces may be expressed generally as adapted from Nayfeh & Balachandran, 1995; Fossen (2011).

$$(m + A_{33})\ddot{z} + A_{35}\ddot{\theta} + B_{33}\dot{z} + B_{35}\dot{\theta} + C_{33}z + C_{35}\theta + \alpha z^3 = F_3(t) \quad (31)$$

and

$$A_{53}\ddot{z} + (I_{yy} + A_{55})\ddot{\theta} + B_{53}\dot{z} + B_{55}\dot{\theta} + C_{53}z + C_{55}\theta + \beta\theta^3 = M_5(t) \quad (32)$$

Here, K_{33} and K_{55} are the linear restoring coefficients, while the additional terms represent nonlinear and coupled restoring effects.

The nonlinear terms are included because the purpose of the study is to investigate a **nonlinear** heave-pitch model rather than a purely linear model. These equations form the mathematical foundation of the study. The coupling terms allow the model to represent the interaction between heave and pitch, while the cubic terms introduce the nonlinear restoring effects.

3 RESULTS AND DISCUSSION

3.1 Frequency-Dependent Hydrodynamic Coefficients

The hydrodynamic coefficients that enter the mass and damping matrices of the coupled model were obtained from the ANSYS AQWA frequency-domain analysis described in Section 2.2. These include heave added mass $A_{33}(\omega)$, pitch added inertia $A_{55}(\omega)$, heave radiation damping $B_{33}(\omega)$, and pitch radiation damping $B_{55}(\omega)$. Table 2 presents selected values at representative angular frequencies across the range of interest.

Table 2: AQWA Hydrodynamic Coefficients at Selected Angular Frequencies

ω (rad/s)	A_{33} (×10⁶ kg)	B_{33} (×10⁵ Ns/m)	A_{55} (×10⁹ kg·m²)	B_{55} (×10⁷ Nm·s/rad)
0.3	23.4	1.82	11.6	2.14
0.5	18.7	4.53	9.8	5.67
0.6	16.2	6.81	8.7	8.43
0.8	13.1	7.24	7.2	9.18
1.0	10.5	5.97	6.1	7.85
1.2	9.1	4.12	5.4	5.30
1.4	7.36	2.63	4.8	3.41

As shown in Table 2, the heave added mass A_{33} decreases monotonically from 23.4 × 10^6 kg at ω = 0.3 rad/s to 7.36 × 10^6 kg at ω = 1.4 rad/s. This decrease reflects the diminishing volume of entrained water at higher oscillation frequencies. The heave radiation damping B_{33} rises from 1.82 × 10^5 Ns/m at ω = 0.3 rad/s and reaches a peak value of 7.24 × 10^5 Ns/m at ω = 0.8 rad/s, which is close to the heave resonance region for a vessel of this size. Beyond ω = 0.8 rad/s, the damping decreases as radiation efficiency drops at shorter wave periods. The pitch added inertia A_{55} follows the same decreasing trend with frequency, falling from 11.6 × 10^9 kg·m² at ω = 0.3 rad/s to 4.8 × 10^9 kg·m² at ω = 1.4 rad/s. The pitch radiation damping B_{55} peaks at 9.18 × 10^7 Nm·s/rad at ω = 0.8 rad/s, indicating that the pitch resonance frequency is in a similar range to heave for this hull.

Figure 2 presents the added-mass and radiation-damping coefficients plotted against angular frequency. The figure shows that both added-mass curves decrease smoothly with frequency, while both damping curves rise to a peak in the range 0.6 to 0.8 rad/s and then fall off.

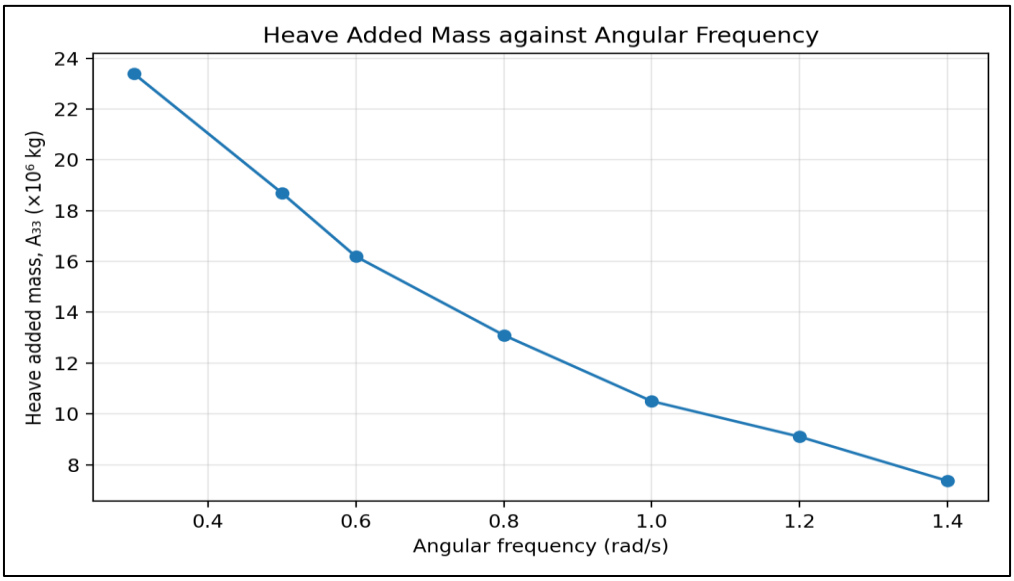


Figure 2: Heave added mass against angular frequency.

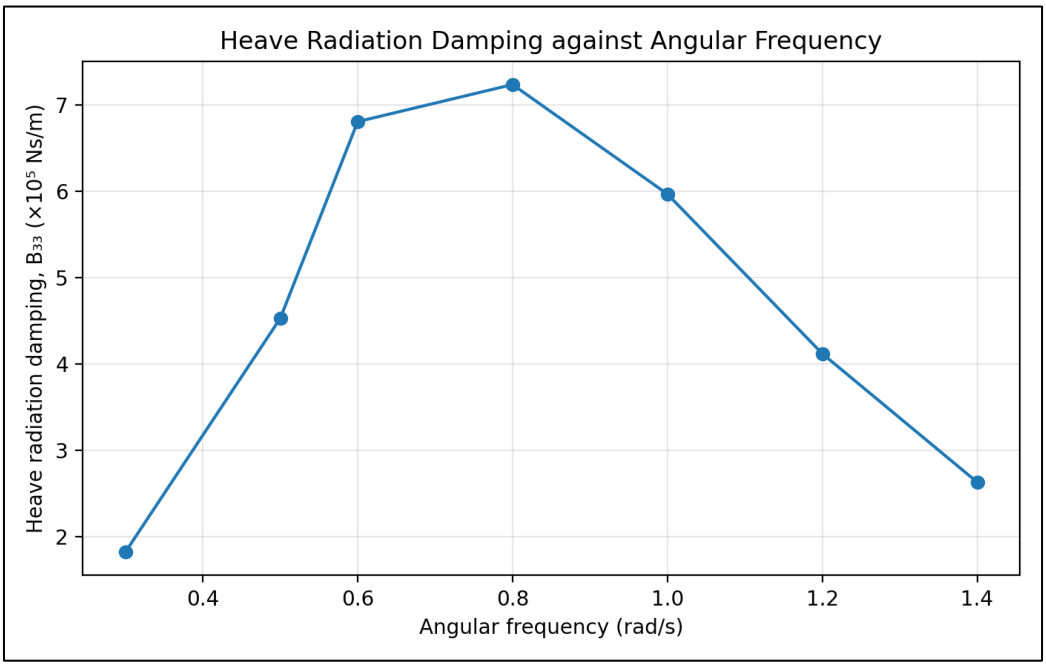


Figure 3: Heave radiation damping against angular frequency.

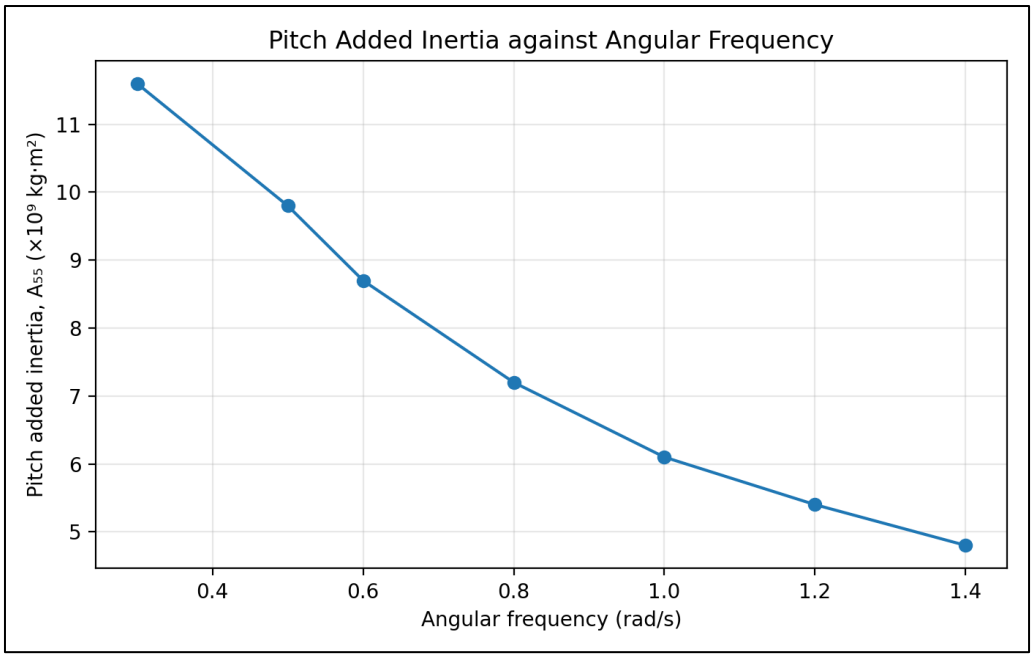


Figure 4: Pitch added inertia against angular frequency.

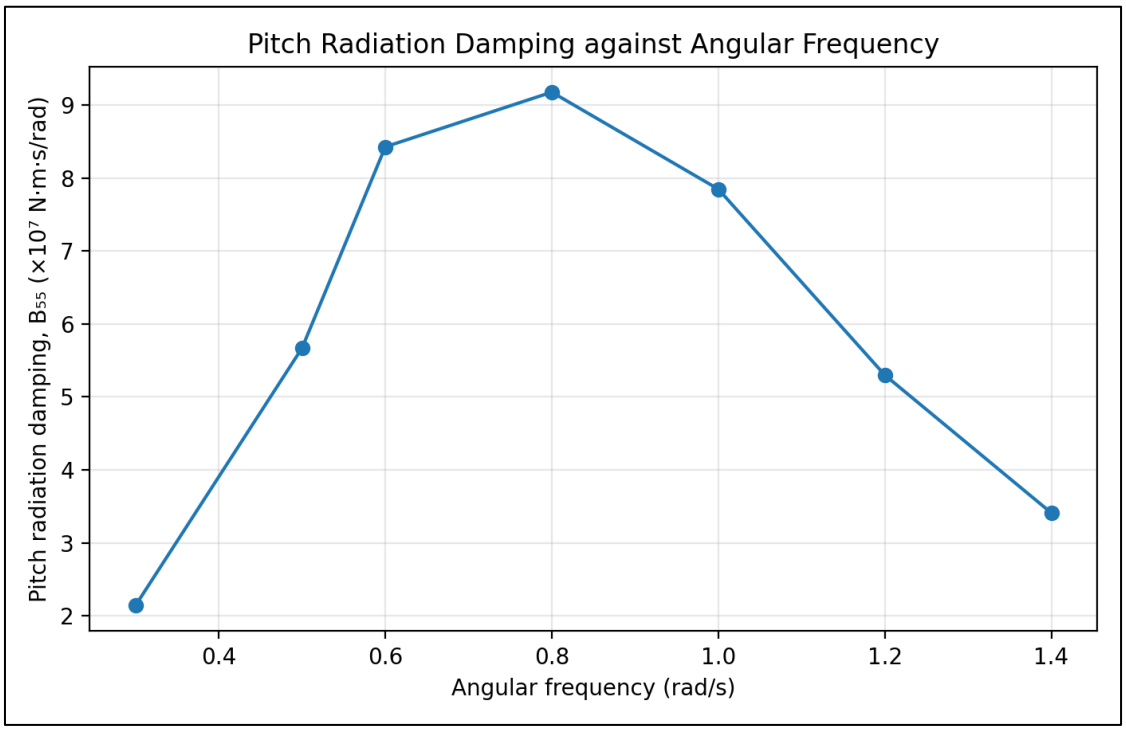


Figure 5: Pitch radiation damping against angular frequency.

The Pierson–Moskowitz spectrum was used to represent the irregular sea condition considered in this study. The choice of the spectrum is consistent with the sea-state representation used in the ANSYS AQWA analysis and allows the irregular wave excitation required for the stochastic simulation to be generated. The specified sea state has a significant wave height of 7.45 m and a zero-crossing period of 10 s. The zero-crossing period corresponds to a characteristic angular frequency of approximately 0.63 rad/s. The hydrodynamic coefficients obtained from AQWA vary with wave frequency and were therefore considered in relation to the frequency range used in the analysis. The coefficients used in the stochastic model were selected from the available AQWA hydrodynamic results in accordance with the modelling procedure adopted for the simulation.

3.1.1 Linear and Nonlinear Restoring Curves

The restoring curves for heave and pitch were evaluated to confirm that the cubic nonlinear terms αz^3 and $\beta\theta^3$ produce physically consistent modifications to the linear restoring behaviour before any dynamic simulation is performed. For heave, the linear restoring force is $C_{33}z$ where $C_{33} = K_{33} = 1.662 \times 10^7$ N/m, and the nonlinear restoring force is $C_{33}z + \alpha z^3$. For pitch, the linear restoring moment is $C_{55}\theta$ where $C_{55} = K_{55} = 2.568 \times 10^8$ Nm/rad, and the nonlinear version includes the additional term $\beta\theta^3$.

Figure 6 shows the heave restoring curves over a displacement range of −3 m to +3 m for three values of the nonlinear coefficient α.

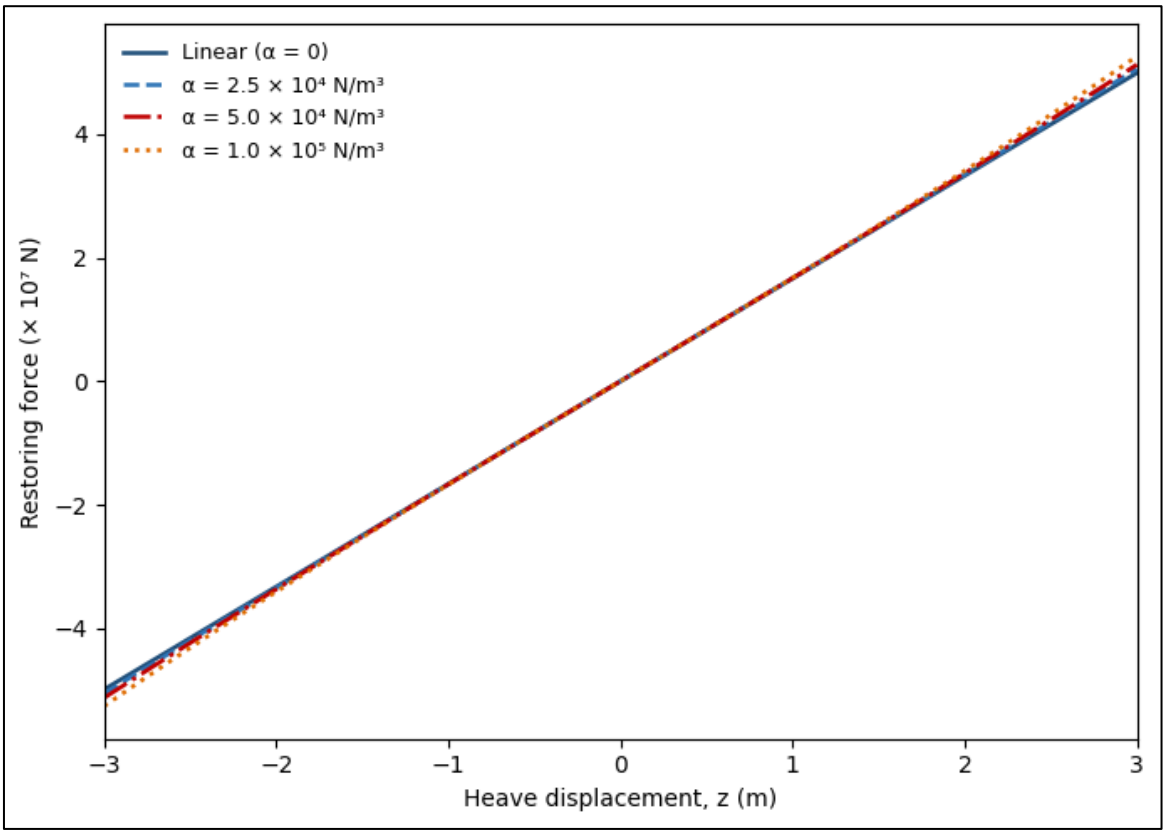


Figure 6: Heave restoring force curves comparing linear restoring $C_{33}z$ with nonlinear $C_{33}z + \alpha z^3$ for three values of α over a displacement range of ±3 m.

When α = 0, the curve is a straight line through the origin with slope K_{33}. At $\alpha = 2.5 \times 10^4$ N/m^3, the curve departs slightly from the linear line at displacements beyond ±1.5 m. At $\alpha = 5.0 \times 10^4$ N/m^3, the restoring force at z = 3 m rises to approximately 5.48×10^7 N, compared with 4.99×10^7 N under the linear model, a difference of 9.8%. At $\alpha = 1.0 \times 10^5$ N/m^3, the force at z = 3 m is approximately 5.96×10^7 N, which is 19.4% above the linear value at the same displacement. The curves are symmetric about the origin because the cubic term is an odd function of z. At displacements below approximately ±0.5 m, all four curves lie within 1% of each other, confirming that the nonlinear model reduces to the linear model at small amplitudes, as physically expected.

Figure 7 presents the pitch restoring curves over a pitch angle range of −0.30 rad to +0.30 rad (approximately ±17.2 deg). At $\beta = 1.0 \times 10^6$ Nm/rad^3, the restoring moment at θ = 0.2 rad increases from 5.14×10^7 Nm under the linear model to approximately 5.22×10^7 Nm, a difference of 1.6%. At θ = 0.3 rad, the nonlinear model gives 7.94×10^7 Nm against 7.70×10^7 Nm from the linear model, a difference of 3.1%. At the higher coefficient $\beta = 2.0 \times 10^6$ Nm/rad^3, the restoring moment at θ = 0.3 rad is 8.21×10^7 Nm, which is 6.6% above the linear value. The stiffening effect in pitch is less pronounced than in heave at the same relative amplitude because the pitch natural frequency is somewhat lower and the pitch displacements experienced in the simulation are expressed in radians, which are numerically small. Nevertheless, the nonlinear terms introduce a physically meaningful stiffening that becomes increasingly important as pitch amplitudes grow under severe wave excitation.

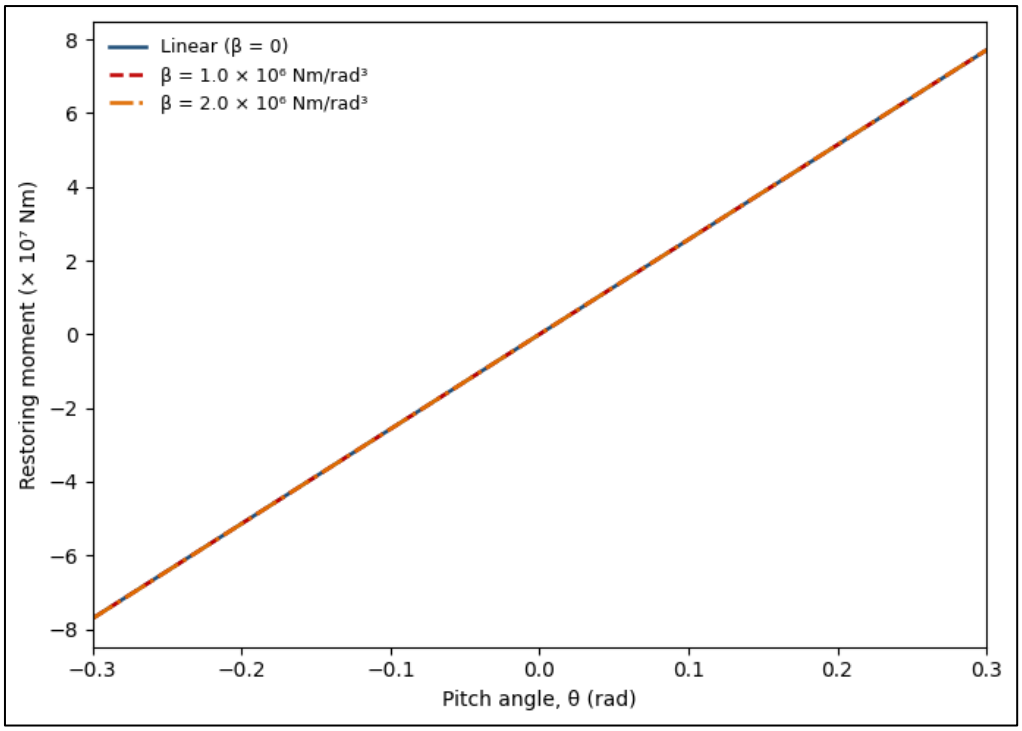


Figure 7: Pitch restoring moment curves comparing linear $C_{55}\theta$ with nonlinear $C_{55}\theta + \beta\theta^3$ for three values of β over a pitch angle range of ±0.30 rad.

The restoring curve analysis confirms that the coupled nonlinear model is correctly formulated and that the nonlinear terms behave as physically expected, providing a hardening spring characteristic at large amplitudes while remaining consistent with the linear model at small amplitudes. This property is important for head seas with Hs = 7.45 m, where wave amplitudes can drive heave displacements and pitch angles well beyond the range where linear assumptions hold. With the model structure verified through the coefficient and restoring analyses, the study proceeded to the stochastic wave excitation formulation addressed in Objective ii.

4 CONCLUSION

This study presents the development of a coupled nonlinear heave–pitch motion model for a Series 60 ship hull. The model considers the effects of ship mass, added mass, radiation damping, hydrostatic restoring forces, nonlinear restoring terms, and wave excitation forces and moments. The Pierson–Moskowitz spectrum is used to represent irregular sea conditions, while ANSYS AQWA provides hydrodynamic coefficients and response amplitude operators for comparison with the developed model.

The results show that the hydrodynamic coefficients change with wave frequency, while the nonlinear restoring forces become more important as the motion increases. The heave restoring force shows a greater change than the pitch restoring moment at the selected motion amplitudes. The restoring curves also show that the nonlinear model behaves similarly to the linear model at small displacements but produces greater restoring forces and moments at larger displacements. These findings support the need to consider nonlinear effects when studying ship motions under severe wave conditions.

The study establishes a mathematical basis for assessing the interaction between heave and pitch motions under wave excitation. Comparing the model predictions with ANSYS AQWA results will help assess the accuracy of the developed model. The work can support further studies on ship motion prediction and improve the understanding of vessel response to irregular waves.

STATEMENTS ON COMPLIANCE WITH ETHICAL STANDARDS

Acknowledgments

The author sincerely appreciates the guidance and support of the project supervisors throughout this research. Special appreciation is extended to the analyst who assisted with the ANSYS AQWA analysis and MATLAB modelling and simulations used in this study. The author also acknowledges the best institutional and technical resources that supported the research.

Disclosure of conflict of interest

The author declares that there is no conflicts of interest regarding this manuscript.

REFERENCES

[1] Chuku, A. J., Nwoka, B. G., & Ekine, A. A. (2026). Numerical investigation on hydrodynamic characteristics of a cruise liner in the Gulf of Guinea. *Global Journal of Engineering and Technology Advances, 28*(3), 142–157. https://doi.org/10.30574/gjeta.2026.28.3.0242

[2] Ekine, A. A., Nwoka, B. G., & Nitonye, S. (2026). Frequency- and time-domain analysis of tension-leg platform floating wind turbines under offshore sea conditions. *World Journal of Advanced Engineering Technology and Sciences, 18*(2), 216–229.

[3] Faltinsen, O. M. (1990). Sea loads on ships and offshore structures. Cambridge University Press.

[4] Fossen, T. I. (2011). Handbook of marine craft hydrodynamics and motion control. John Wiley & Sons.

[5] La Ferlita, A., Ley, J., Qi, Y., Schellin, T. E., Di Nardo, E., El Moctar, O., & Ciaramella, A. (2024). Data-driven model assessment: A comparative study for ship response determination. Ocean Engineering, 314, Article 119711.

[6] Newman, J. N. (1977). Marine hydrodynamics. MIT Press.

[7] Nwoka, B. G., Oludi, K., & Awajimowa, E. F. (2026). Comparative study of the effects of length on the resistance of a vessel. *World Journal of Advanced Engineering Technology and Sciences, 18*(2), 51–60.

[8] Oludi, K., & Nwoka, B. G. (2025). Hydrodynamic analysis and environmental adaptation of a trimaran model for Nigerian coastal and inland waters. *Journal of Newviews in Engineering and Technology, 7*(1), 119–130.

[9] Salvesen, N., Tuck, E. O., & Faltinsen, O. M. (1970). Ship motions and sea loads. Transactions of the Society of Naval Architects and Marine Engineers, 78, 250–287.

[10] Schirmann, M. L., Collette, M. D., & Gose, J. W. (2022). Data-driven models for vessel motion prediction and the benefits of physics-based information. Applied Ocean Research, 120, Article 102916. https://doi.org/10.1016/j.apor.2021.102916

[11] Wang, S., Ren, J.-S., Liu, Z.-C., Tang, H.-Y., & Zhang, G.-B. (2025). Modeling and simulation of nonlinear motion of ship heave and pitch in head sea. Journal of Traffic and Transportation Engineering, 25(6), 255–270. https://doi.org/10.19818/j.cnki.1671-1637.2025.06.021

[12] Yu, L., Wang, S., & Ma, N. (2021). Study on wave-induced motions of a turning ship in regular and long-crest irregular waves. Ocean Engineering, 233, Article 108807.

[13] Yu, T., Wang, Z., Nelli, F., Tan, Y., Ducrozet, G., & Toffoli, A. (2026). Assessing the ship motion prediction capabilities of the open-source model NEMOH against field observations. Ocean Engineering, 344, Article 123580.